Transportation Geotechnics 17 (2018) 33–40

Contents lists available at ScienceDirect

Transportation Geotechnics

journal homepage: www.elsevier.com/locate/trgeo

Full scale laboratory testing of ballast and concrete slab tracks under phased cyclic loading

T. Marolt Čebašek[a,*], A.F. Esen[b], P.K. Woodward[a], O. Laghrouche[b], D.P. Connolly[a]

[a] Institute for High Speed Rail and System Integration, University of Leeds, Leeds LS2 9JT, UK
[b] Institute for Infrastructure and Environment, Heriot Watt University, Edinburgh EH14 4AS, UK

ARTICLE INFO

Keywords:
Full-scale cyclic testing
Railway track settlement
Railway track stiffness
Long-term track behaviour
Ballast and concrete slab track

ABSTRACT

Full-scale laboratory-based testing is used to compare the long-term settlement performance of a precast concrete slab track section to a ballasted track (with concrete sleepers) resting on a compacted substructure. The railway track substructure is constructed from a 1.2 m deep combined subgrade and frost protection layer, according to modern high-speed rail standards such as those specified in Germany. Phased cyclic loading is then used to simulate the primary loading mechanism of a train after 3.4 million load cycles representing many years' worth of train passages. Displacement transducers, earth pressure cells and accelerometers are employed to determine the permanent settlement, the cyclic displacement, transient stresses and vibrations of the track. The equipment, loading combinations, material properties and experimental displacement results are presented and compared. The results indicate that the ballasted track experienced 20 times more settlement when compared to the concrete slab track under the same loading conditions, even though the ballasted track was tested at a slightly higher compacted state due to the concrete slab track test being conducted first.

Introduction

It is well known that high-speed railway track design presents many challenges in comparison to conventional speed railways. Currently, both ballasted and concrete slab tracks are being used for high-speed railways worldwide and it is recognised that both forms have advantages and disadvantages. It is generally known that the initial cost of installation of ballasted track is cheaper in comparison with concrete slab track but on the other hand the maintenance costs of ballasted track are higher [1,2]. Nevertheless, ballasted track has been continuously developed since the beginning of the railways and it is still the most common track system used today. Due to the overall poor performance of ballast for increased train speeds, the use of concrete slab track has attracted a lot of attention and various slab track forms have been produced and tested in recent years.

Full-scale testing has been used to investigate the performance of various parts of the railway track structure. For example, full-scale model tests with simulated train moving train loads has been developed to explore the dynamic performance and long-term behaviour of concrete slab tracks [1,3]. In the case of ballasted track, a two-layer railway track model was developed and tested [4]. It was reported that the subgrade plays an important role in the global track stiffness and hence the deterioration of vertical track geometry [5]. It was noted that a low track stiffness value can result in a flexible track with poor load distribution and a high track stiffness value can cause greater dynamic overloads on the rail with increased train-track interaction forces [6,7] leading to rail defections such as corrugation.

One of the main causes of track deterioration is the settlement of the substructure. An accumulative deformation prediction method under repeated moving loads has been proposed by Bian [8]. The post-settlement is influenced by the number of loading cycles and self-weight of the embankment. The results from the full-scale model testing shows that the dynamic loading has a significant contribution.

Various settlement models have been developed [9–14]. It was shown that they all follow a similar pattern in describing the behaviour of ballast settlement under cyclic loading. Many authors introduced into their model two phases of the track settlement. The first part is a nonlinear relationship between settlement and number of cycles and the second phase tends to be linear [15]. Selected settlement models were presented by Abadi [16] who compared some current empirical ballast settlement models against experimental data obtained from a section of track consisting of a single sleeper bay. The settlement of the track also depends on the properties of the material used for the subgrade. Long-term deformations of fine and coarse-grained soils have been reported in many laboratory and field tests; however, the number of loading cycles was limited [17].

* Corresponding author.
E-mail address: t.marolt@leeds.ac.uk (T. Marolt Čebašek).

https://doi.org/10.1016/j.trgeo.2018.08.003
Received 30 June 2018; Received in revised form 13 August 2018; Accepted 31 August 2018
Available online 01 September 2018

Shakedown approach has been used for structural analysis of unbound materials. A model of permanent deformation behaviour of unbound granular materials was introduced in [18]. It expresses the accumulated permanent axial strain at any given number of cycles as a function of applied stresses ratio and the length of the stress path. A series of laboratory tests using a triaxial cell were conducted on two unbound granular material types by varying simultaneously the axial stress and the radial stress, which showed that the plastic strain behaviour was stress-path dependent [19].

The initial compaction stage (plastic strain e_p) of the concrete slab track are often described by:

$$e_p = aN^b \tag{1}$$

where a and b are constants.

The effect of the train load on track settlement can then be found from:

$$e_p = a\left(\frac{\sigma_d}{\sigma_s}\right)^m N^b \tag{2}$$

where σ_d and σ_s are the deviator and compressive strength respectively and m is a material parameter and N is the number of cycles.

After this point plastic settlement essentially reaches a steady state with further train loading and hence the track settlement rate reduces dramatically.

The aim of this study is to compare the settlement that occurs under the same loading regime with similar highly compacted substructures, representative of international standards for a ballast and concrete slab track, and hence contribute to the international literature comparing the direct shakedown behaviour of concrete slab track and ballasted track. First, the full-scale Geo-pavement and Railways Accelerated Fatigue Testing (GRAFT-2) facility is briefly presented in Section "Laboratory testing", followed by the subgrade, slab track and ballasted track characteristics. In Section "Testing methodology for static and cyclic testing", the testing methodology is described including both the static and dynamic loading methods. Part of the experimental results are presented and analysed in Section "Analysis". Finally, concluding remarks are summarised in Section "Conclusions".

Laboratory testing

In this section, the experimental setup, used materials and their associated properties are described.

Experimental setup

The full-scale GRAFT-2 facility situated at Heriot-Watt University is shown in Figs. 1 and 2. It was used to test a section of concrete slab track and ballasted track with concrete sleepers as indicated in Fig. 2.

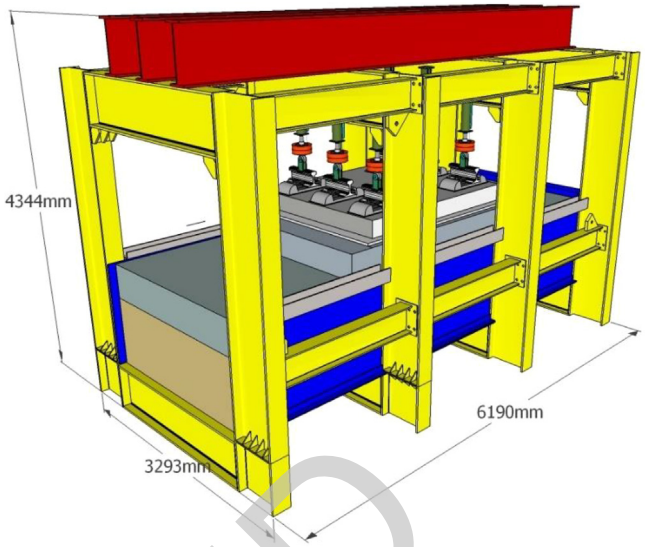

Fig. 2. Dimensions of GRAFT-2 facility.

The main purpose of this test facility is to assess and characterise the short and long-term performance of different track forms and their interaction with the formation. The accelerated testing approach mimics many years of train passages in just a few days of testing. It operates by using six independent hydraulic actuators loading three full-sized sleepers, on ballasted track, or a concrete slab track with three built-in sleepers, to simulate the passage of a moving train (by phased loading), with each piston applying loads on a given rail segment.

Subgrade

The depth of the substructure, including the subgrade and the Frost Protection Layer (FPL), was 1.2 m. The substructure consisted of a well-graded granular limestone according to ASTM [20] and its granulation is presented in Fig. 3. The optimal moisture content was determined by a modified Proctor compaction test, carried out at the geotechnics laboratory at Heriot-Watt University, and its value was 4.5%. The effective internal friction angle ϕ' was measured to be 35° at the optimum moisture content, the specific gravity parameter was 2.69 and the maximum dry density was 22.2 kN/m^3. It was assumed that the moisture content did not change during the testing period.

The height of the subgrade was 800 mm and the thickness of the FPL was 400 mm, as presented in Fig. 4. They correspond to the German ZTVE-StB 94 standard [21]. In this standard the deflection modulus E_{v2} should be at least 120 MN/m^2 for the FPL and at least 60 MN/m^2 for the subgrade. The deflection modulus E_{v2} was verified using a static plate

a) b)

Fig. 1. (a) Slab track test and (b) Ballasted track test in GRAFT-2 facility.

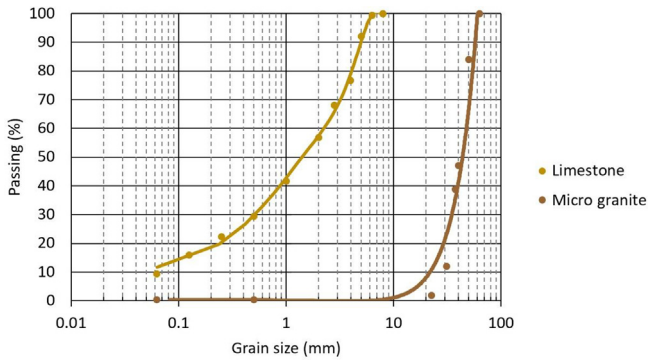

Fig. 3. Sieve analysis for limestone and micro granite.

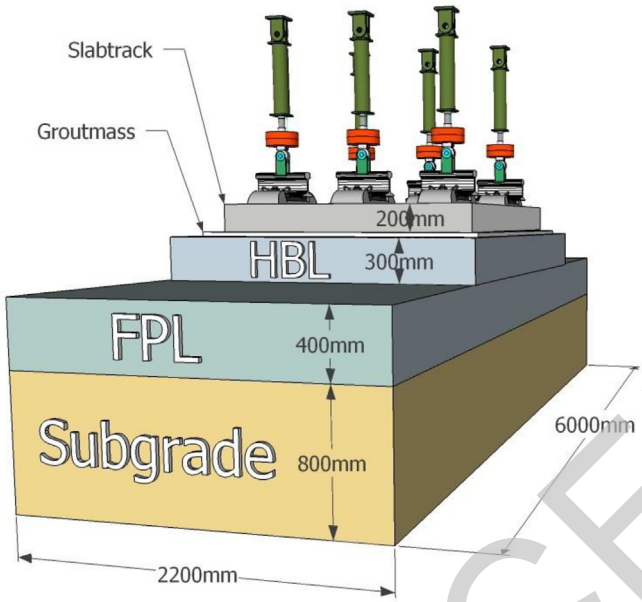

Fig. 4. Model of substructure and super structure incorporated in the test facility for concrete slab track test.

load test in accordance with DIN-18134 standard [22]. The coefficient of permeability (k) should be between 10^{-5} m/s and 10^{-4} m/s for the FPL and relative density (D_r) within 98–100% for the FPL and subgrade. In this paper the E_{v2} value of the FPL was estimated through the plate load test (Eq. (4)) to be 133.55 MN/m^2, and E_{v2}/E_{v1} was 1.42, the permeability k was evaluated through the permeability test and was found to be 10^{-5} m/s and D_r was 100%. Further laboratory tests found the E_{v2} value of the subgrade to be 67.71 MN/m^2, E_{v2}/E_{v1} = 1.55 and D_r = 98%.

The Young's modulus of the subgrade can be found using the following general equation for plate loading testing:

$$E_{PLT} = \frac{2P(1-\nu^2)}{\pi r \delta} \quad (3)$$

where E_{PLT} is Young's elastic modulus; P is applied load; r = radius of plate; ν is Poisson's ratio; and δ is deflection of plate.

To build the substructure, the sand was compacted using a forward/reverse plate compactor. In order to achieve an effective compaction, the sand was compacted into layers of 200 mm thickness. The compaction level was set based on a correlation between the CBR values, which were obtained via dynamic cone penetrometer tests, and E_{v2} values which were obtained using the plate load tests. The right level of compaction was essential to achieve the required stiffness of the subgrade and FPL layers.

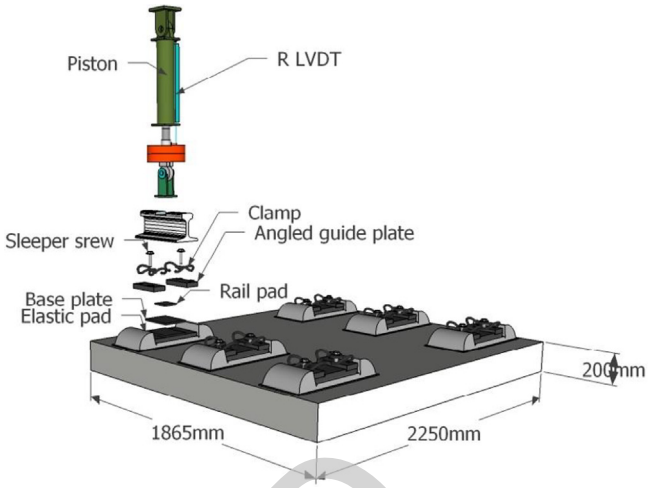

Fig. 5. Tack system and loading configuration.

Concrete slab track

While the substructure consists of a subgrade and a FPL, the superstructure consists of a Hydraulically Bonded Layer (HBL), grout mass and a concrete slab track segment and its associated components, as shown in Fig. 4. The HBL thickness was 300 mm and it was made from concrete C10/12 with a cement intake of 110 kg/m^3, an average modulus of elasticity (E) of approximately 7500 MN/m^2; E for the concrete was 20,000 MN/m^2. Positioning the slab track segment on the HBL was performed with a slab positioning system that provided a high precision of alignment; a 40 mm gap between the HBL and the concrete slab track itself was left during this process. This gap was then filled with a non-shrinking cement grout mass to bond the slab to the HBL.

In this study a typical (cut) Max Bögl slab track segment was used for the concrete slab track. It was a prefabricated slab made of reinforced concrete C45/55. The dimensions of the tested slab are presented in Fig. 5. The Max Bögl slab can be pre-stressed in the lateral direction and traditional reinforcement is applied in the longitudinal direction. The test specimen comprised three pairs of rail seats which were uniformly integrated longitudinally and transversally. Predetermined breaking points are included to help prevent uncontrolled crack growth; this feature is considered a special characteristic of this particular slab track system. In order to drain surface water, the slab track is manufactured with a 0.5% transverse slope by default.

The rail fastening system was a 300-1; manufactured by Vossloh Fastening Systems. The height was adjustable from 76 mm to −4 mm. The static stiffness of the lower elastic pad was approximately 22.5 kN/mm and the dynamic stiffness was approximately 40 kN/mm. The static stiffness of the upper rail pad was approximately 600–700 kN/mm and the dynamic stiffness was approximately 1600–1800 kN/mm. The cut rail segments used in the slab track test were 60E1 (UIC 60). The HBL was cast on the top of the FPL which corresponded to the basic minimum parameters mentioned above.

The concrete slab track was subjected to more than 3 million load cycles and there was no evidence of fatigue of the slab itself. However assessing the fatigue strength due to ageing of the system was not possible in these tests due to the track system only being tested over a short 13 day period which was all that was necessary to apply the predetermined number of load cycles.

Ballasted track

The ballasted track test followed the concrete slab track test (i.e. ballast was placed after removal of the concrete slab track and the HBL). Therefore for the ballasted test, the main part of the substructure

Fig. 6. Geogrid placed at the interface between the ballast and the substructure.

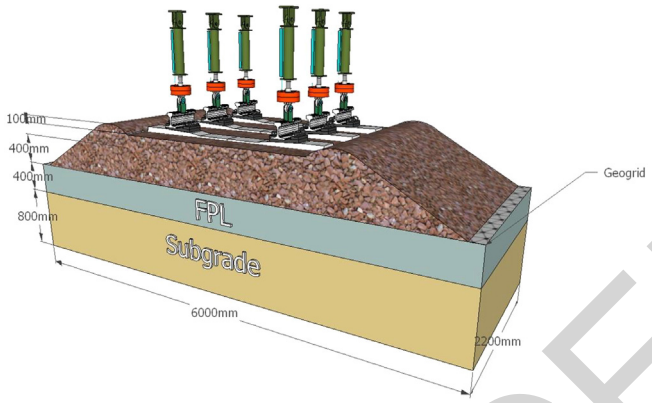

Fig. 7. Layout of ballasted track and substructure.

remained unchanged and only the superstructure was fully replaced. The top 50 mm of the FPL was however replaced between the tests due to the disturbance caused by removing the HBL. This thin replaced layer was compacted to the same level as before. A TX190L geogrid was laid over the FPL as shown in Fig. 6. The geogrid was used to reduce penetration of ballast into the substructure geomaterial. The results obtained in a study from the University of Nottingham Railway Test Facility indicated the potential reduction in settlement achieved when an appropriate geogrid is installed under the ballast [23,24]. The ballast was placed in 100 mm intervals to reach 400 mm thickness immediately under the sleepers as shown in Fig. 7. An electric compactor with 400 mm × 320 mm plate was used to compact each 100 mm of the ballasted layer to reach a relative compaction. The bulk density after compaction was 16 kN/m^3. In this study standard G44 sleepers were positioned at 650 mm spacing.

The ballast consisted of micro-granite with a moisture content of 0.5% and with the gradation shown in Fig. 3. The same lower elastic pads from the slab track test were used as rail pads for the ballasted track test. The 'fast clip' fastening system by Pandrol was used to lock the rails to the sleepers. The cut rail segments used in the ballasted track test were BS113A (56E1) – since the bending stiffness of the rail is not being used this was thought not to affect the results of the test. The ballasted track was tested for more than 3 million cycles following the same procedure carried out as for the concrete slab track test.

Testing methodology for static and cyclic testing

The appropriate redistribution of the axle load for the initial static tests over the ballasted and concrete slab tracks was applied by considering the full axial load. This was simulated by assuming that approximately 50% of the load would pass directly into the middle sleeper with just a quarter going to each adjacent sleeper. This approach was based on the use of the approximate model of a beam on an elastic foundation. The effects caused by wheel rail irregularities were not considered [25].

For the cyclic test case however the above-mentioned redistribution was not followed. Instead, the full load was used on each sleeper to represent a worst case scenario and allow direct comparisons between the concrete slab and ballasted tracks, i.e. the same loading case with very little load redistribution due to the high subgrade stiffness (Table 1 shows the load distribution for both static and cyclic test cases). It should be noted that the axle load distribution should only be considered as an approximation to the real load distribution. In total, four tests were carried out, two static tests and two cyclic tests. In the cyclic tests, the sequential loading was applied with a time phase Δt between two neighbouring actuators in the track direction given by:

$$\frac{\Delta s}{v} \tag{4}$$

where Δs (m) is the distance between two neighbouring actuators in the track direction and ν (m/s) is the assumed train speed. However, the loading frequency in GRAFT-2 only represents repeated single wheel loading on the rail segment and is therefore an approximation of real track loading conditions.

The principle of the sequential loading method was proposed and validated by using the dynamic substructure method [26]. The effect of the train speed on the soft subgrade is not considered within this testing. Moreover, the train speed is well below the track critical velocity [27,28].

The cyclic/dynamic tests were carried out with two different loads and frequencies. The first case, termed Dynamic I, was performed with a frequency of 5.6 Hz and lower forces as indicated in Table 1. The second case, Dynamic II, was carried out with a lower frequency, 2.5 Hz, and higher forces (see Table 1). The primary limitation was the capacity of GRAFT-2. Frequency of 5.6 Hz was calculated based on the distance between two bogies on the same rolling stock. Higher frequencies than 5.6 Hz were not feasible to reach. On the other hand, 2.5 Hz was the frequency at which the GRAFT-2 performed the best in terms of higher loads.

The phased loading on the three sleepers is indicated in Fig. 8 and as mentioned above it should only be considered as an approximation to the primary loading mechanism (primary cycle) for the passage of a pseudo train wheel on stiff ground (i.e. for the 5.6 Hz in Dynamic I, a pseudo train wheel passing at 100 m/s (360 km/h).

Table 1
Loading sequences of the ballasted and concrete slab track tests.

TEST	Axle load on middle sleeper (kN)	Redistribution of load per actuator (kN)	Redistribution of load over the sleeper (%)	Frequency (Hz)	Time interval between sleepers (s)	Duration
Static I	63.77	15.94, 31.88, 15.94	25, 50, 25	N/A	N/A	620 s
Static II	83.34	20.84, 41.69, 20.84	25, 50, 25	N/A	N/A	788 s
Dynamic I	117.72	58.86, 58.86, 58.86	100, 100, 100	5.6	0.0065	1.17×10^6 cycles
Dynamic II	166.71	83.34, 83.34, 83.34	100, 100, 100	2.5	0.0065	2.20×10^6 cycles

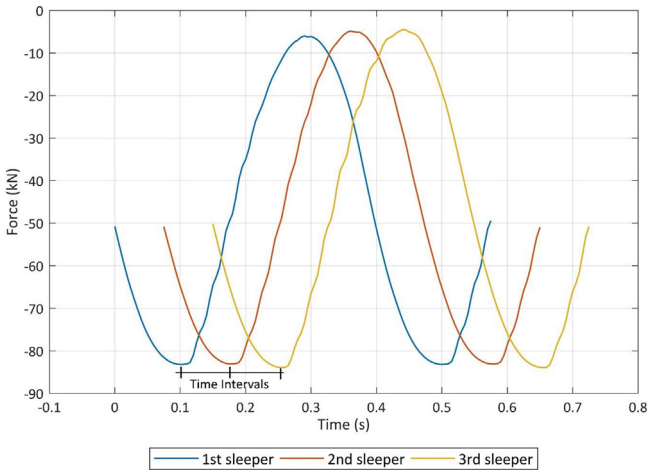

Fig. 8. Time interval of sequential loading in one cycle.

For data acquisition, 31 out of 32 active channels were used to acquire the data from the tests with a sampling rate of 200 Hz, i.e. 80 data points for each cycle at 2.5 Hz and 36 data points for each cycle at 5.6 Hz. In order to investigate the pressure changes in the subgrade and FPL, five pressure cells were situated at different locations and depths (these pressure readings will be published in a later paper). For controlling the deflection of the pistons, as well as to set limits in terms of loads (kN) and displacement (mm), 12 channels were used on the actuators; six load cells and six linear variable differential transducers (LVDTs). To measure the deflection and total settlement, four 12 mm high-precision LVDTs and three 75 mm LVDTs were used at key locations on the slab for the concrete slab track test and on the sleepers for the ballasted track test. Lastly, three accelerometers were positioned to measure the vibration of the track. In terms of this paper, the displacement under loading and the shakedown settlement are presented.

Analysis

In this section, results related to the static and cyclic/dynamic tests are presented and analysed.

Static compressive loading

A static compressive load was applied to the slab track (ST) and ballasted track (BT) in the same manner. At the beginning (Static I), a load of approximate 16 kN was applied for 618 s and then (Static II) a load of 21 kN was applied for 788 s on adjacent sleepers, as shown in Fig. 9. The exact values of the applied forces in the experiment on the

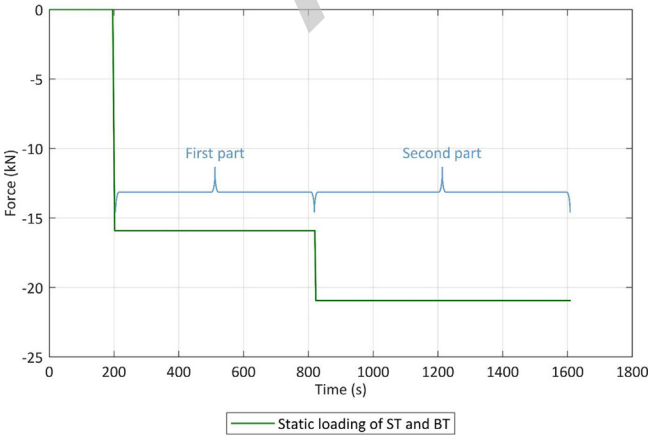

Fig. 9. Force vs time for ballasted and concrete slab track.

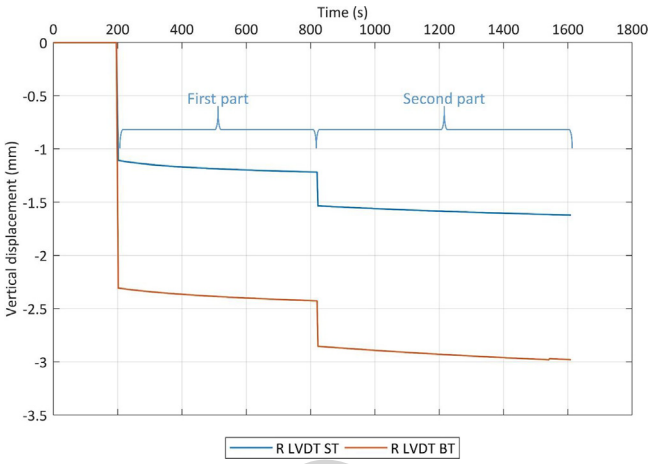

Fig. 10. Vertical displacement vs time on the top of rail for ballasted (R LVDT ST) and concrete slab track (R LVDT ST).

sleeper or slab are presented in Table 1.

The displacement and settlements on the surface of the sleepers for the ballasted track and on the surface of the slab for concrete slab track were monitored by the surface-LVDTs (S LVDTs). The vertical displacements on the top of rail for both tracks were monitored by the rail-LVDTs (R LVDTs). The results from selected LVDT measurements are presented in Figs. 10 and 11. As expected, it can be seen in Fig. 10 that the displacements of the ballasted track are higher due to the unbound nature of the ballast. In addition Fig. 11 also confirms that the slab track displacements, due to higher loads, are still negligibly small owing to the high rigidity of the concrete slab track. However, for the ballasted track, higher displacements are observed when the load was increased due to the lower stiffness of the unbound ballast support system.

As previously mentioned, the same lower elastic pads were used in both the slab and ballasted track tests. When the effect of the subgrade and ballast displacements are subtracted the displacements of the rails were similar in both track cases as shown in Fig. 12 showing that the effect of the different rail sections was negligible; this also serves as a quick check of the rail measurements from one track set up to the next.

Cyclic/dynamic loading

The magnitude of individual peak loads and the cyclic nature of the train loading are two important factors that influence the behaviour of the track settlement [29]. Trains typically subject the track to repeated cyclic/dynamic phased loading and hence the track's principal stresses

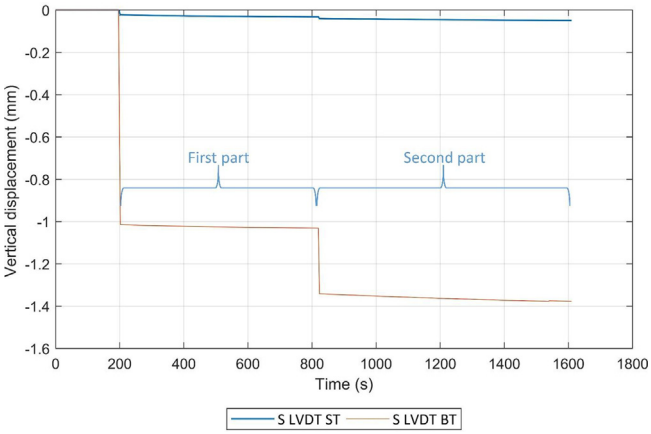

Fig. 11. Vertical displacement vs time on the top of sleeper for ballasted track (S LVDT ST) and on top of the slab for slab track (S LVDT ST).

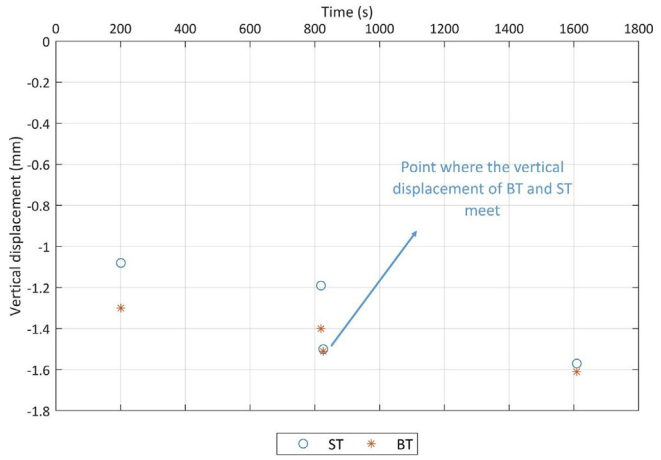

Fig. 12. Vertical displacement on the surface of rail for ballasted track (BT) and for slab track (ST) without displacements in the ballast and subgrade, respectively.

rotate due to the constantly changing load direction. This can lead to changes in the settlement behaviour of the track and its underlying substructure. Simulating the phased loading of the track structure, to allow principal stress rotation, is a key element of the testing capability of GRAFT-2. The discrete nature of the ballast particles highlight the importance of simulating principal stress rotation. It should be noted that in the case of the concrete slab track, its high rigidity will change the nature of the stress rotations in the subgrade when compared to the ballasted track.

The key risk associated with both the ballasted and the concrete slab track is the differential settlement under repeated loading – in the latter case significant maintenance may be required to prevent concrete cracking. This settlement is influenced by properties like the accumulative tonnage (number of trains and axles), the loading period and the characteristic material parameters and conditions of the track structure.

In order to investigate the permanent deformation of the concrete slab track and ballasted track studied in this paper, repeated phased axle loads were applied using the GRAFT-2 facility.

As previously mentioned, two cyclic/dynamic tests were performed successively (Table 1). The first one was performed with a varying peak load of 58.86 kN at 5.6 Hz and the second one with a varying peak load of 83.34 kN at 2.5 Hz. As shown in Fig. 13, the load amplitudes and sinusoidal signals at the two frequencies show similar patterns for the concrete slab track and the ballasted track tests.

During testing the cyclic load cannot be allowed to go to zero

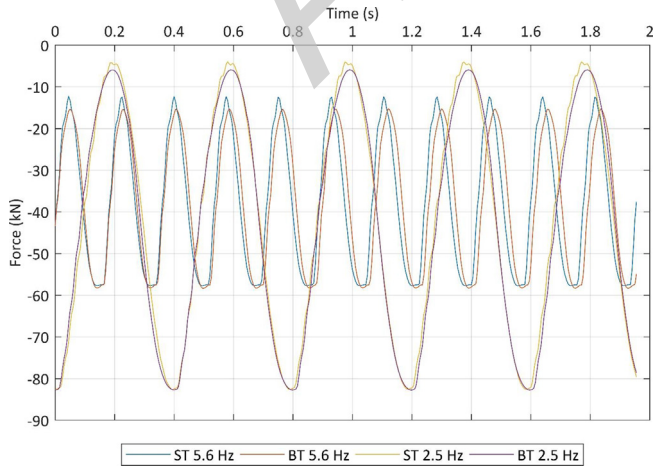

Fig. 13. Force vs time for ballasted track (BT) and concrete slab track (ST) at 2.5 Hz and 5.6 Hz.

Table 2
CBR values of subgrade and FPL layers during the compaction of the sand and after completing the concrete slab track and the ballasted track tests.

CBR Test Time	CBR value	R^2
During construction of Substructure -Subgrade	31.76	0.9335
During construction of Substructure -FPL	43.36	0.8727
After Removal of Slab - FPL	120.56	0.9921
After Removal of Ballast - FPL	120.56	0.9944

because a tensile drift of the actuator would then occur which might result in the actuator trying to lift off the sleeper or slab – in the latter case the slab would then try to lift off the HBL or the FPL which might result in damage to the HBL. Therefore, sinusoidal loading ranging between 12 kN and 58.86 kN at 5.6 Hz and between 4 kN and 83.34 kN at 2.5 Hz was adopted. The loads of 12 kN and 4 kN represent seating loads to prevent this lifting of the slab or sleepers at any instant of the cyclic loading.

Table 2 indicates the CBR values measured using the Dynamic Cone Penetrometer (DCP) at various times during the testing. In order to identify the level of the compaction, six DCP tests were performed at different locations in the testing rig for each layer. The penetration depth of the cone was approximately 100 mm for each test. The tests were performed at each compaction layer during construction which provided the CBR values for both the subgrade and FPL. After completion of the slab track tests, the superstructure was removed and then CBR values were collected on the FPL surface. Hence, the ballast was placed and after completing the ballast tests, the ballast and the geogrid were removed. The DCP tests were then performed again. In this way, the stiffness change after both the slab and the ballast tests were obtained.

As it can be seen clearly from Table 2, the stiffness of the substructure increased significantly during the slab track tests to high values. On the other hand, the additional stiffness rise during the ballast track tests is small as the soil was already stiffened during the concrete slab track tests. However it should be noted that the high CBR results obtained (after the first set of cyclic loading) will not be as reliable as the CBR values taken during the construction of the subgrade. This is because of the difficulties identifying the exact movement of the cone when the penetration is very low (i.e. less than a few millimetres as small change can lead to large variations in the CBR value).

The results of the cumulative settlement of the concrete slab track and the ballasted track are presented in Fig. 14.

The figure shows that the cumulative settlement in the ballasted track is approximately 20 times higher in comparison to that of the

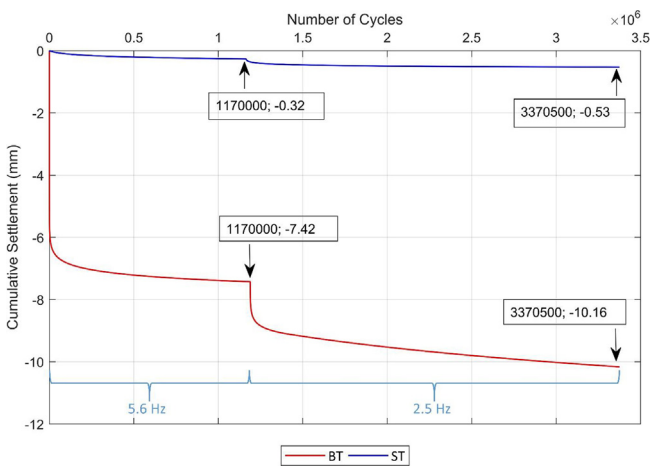

Fig. 14. Cumulative settlement of concrete slab track (ST) and ballasted track (BT) vs number of cycles.

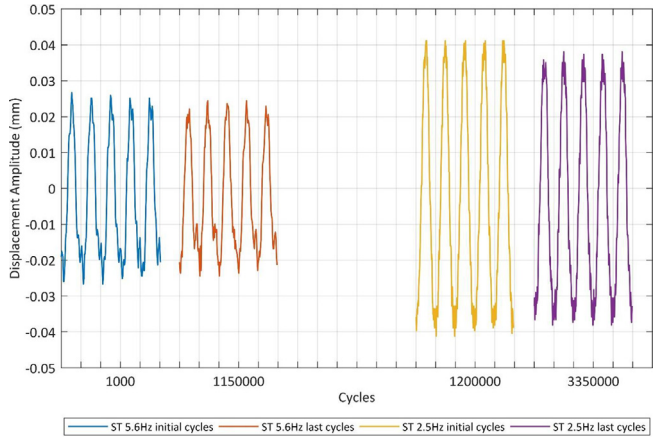

Fig. 15. Amplitude of concrete slab track at the beginning and at the end of the 5.6 Hz and 2.5 Hz cycles, respectively.

concrete slab track under the same loading conditions. This is confirmed in both loading aspects of the ballasted track test, i.e. at 5.6 Hz and 2.5 Hz cyclic frequencies which, as shown in Fig. 14, have two stages of cumulative settlement.

The second increase in the cumulative settlement (particularly evident in the ballast test) clearly highlights, that in a real track loading environment, recommencement of plastic deformation (ballast and/or subgrade) can occur due to increases in the peak load even when a resilient state has already been achieved at the lower peak loading level.

The penetration of ballast into the subgrade during the ballast test was likely reduced by the presence of the geogrid; which was placed at the interface between the subgrade and the ballast layer. Although the measured ballasted track settlement includes both the ballast and the substructure (FPL and subgrade) deformation, it can be reasonably assumed that there was relatively little settlement within the substructure, due to the high initial stiffness of the formation after the concrete slab track test, when compared to the settlement generated within the ballast layer itself [30,31] during loading.

In Figs. 15 and 16 the displacement amplitudes of the ballasted track and the concrete slab track are presented at the beginning and at the end of the first part of the cyclic loading at a frequency of 5.6 Hz and also for the second part of the cyclic loading at a frequency of 2.5 Hz. The midpoint of the cycle is set to 0 for convenience. The amplitudes are seen to be reducing throughout the testing in comparison to the start of the cyclic loading, showing that the track is stiffening with load application. The displacement amplitude of the concrete slab track

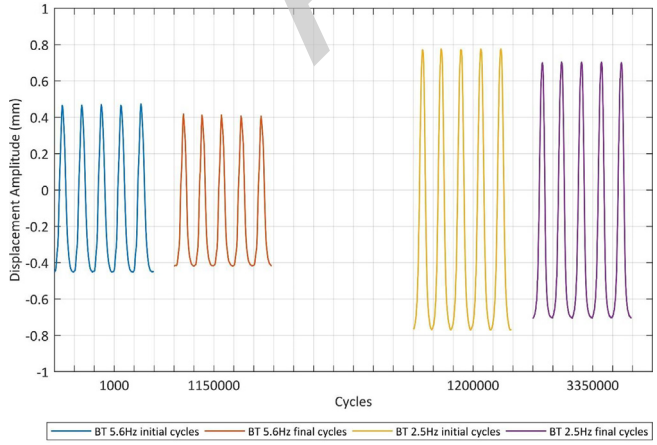

Fig. 16. Amplitude of ballasted track at the beginning and at the end of the 5.6 Hz and 2.5 Hz cycles, respectively.

and ballast track is approximately 9% lower at both frequencies; however there is a significant difference between the amplitude sizes at different the frequencies due to the differing load amplitude.

The reason for the smoothness of each cycle relates to the precision of the LVDTs and the load cell data acquisition system which is able to capture significant parts of each load cycle. As can be observed, the overall displacement magnitude of the cycles for the ballasted track is at least 20 times greater than the magnitude of the concrete slab track cycles. It should be noted however that this difference is in part due to the size of the test specimens (i.e. the effect of the boundary conditions in GRAFT-2).

The ballasted track settlement is a result of the densification due to plastic particle rearrangement (thought to be mainly ballast) under repeated cyclic loading, leading to the penetration of the sleepers into the ballast, and ballast volume changes due ballast breakage and abrasive wear. Although reduced it may also be the result of some potential penetration of the ballast into the underlying FPL in spite of the presence of the geogrid although as discussed earlier this was not thought to be significant due to the high initial ground stiffness, i.e. compactive state. The settlement of the concrete slab track under cyclic loading was very low again indicating the high initial compactive state of the FPL and subgrade.

Excessive and rapid accumulation of plastic deformation in ballast leads to track settlement and hence track geometry issues resulting in the need for track maintenance. This can be achieved either through tamping whereby the ballast matrix is disturbed (by the vibrating tamping tines used to correct the track geometry) or through stone blowing whereby disturbance is significantly reduced by comparison. In the case of a substructure with low bearing capacity, the subgrade is the main source of settlement but if the substructure has a relatively high bearing capacity, then the ballast layer represents the main source of the settlement. At high line speeds the high acceleration levels in the ballast may result in further track settlement as the unbound ballast starts to decompact due to vibration; however this would not be the case in the concrete slab track case as it is a bound system.

Conclusions

In this work, full-scale laboratory testing of two different types of railway track types, namely concrete slab track and ballasted track, were carried out under the effect of two different axle loads, applied statically and then cyclically/dynamically. The load was transmitted through full-scale three-sleeper sections resting on a 1.2 m deep subgrade and frost protection layer, built according to high-speed rail standards. The dynamic loads were applied via 6 independent actuators by phased cyclic loading to simulate moving axle loads.

It was clearly observed that the concrete slab track performed significantly better in terms of cumulative settlement and peak rail displacements when compared to the ballasted track. The main reason for the observed higher settlement of the ballasted track was thought to be due to the unbound nature of ballast, rather than due to the settlement of the substructure (the substructure was well compacted prior to the concrete slab track test and was even more compacted prior to the ballasted track test – i.e. high CBR values were recorded after the slab test). It is therefore possible that had the ballasted track been tested first it would have experienced an even higher track settlement.

The main concluding remarks drawn from the testing results presented in this paper are as follows:

- Both the ballasted and concrete slab track followed typical shake-down periods even at the high formation stiffness.
- The total settlement of the concrete slab track is significantly lower than that of the ballasted track under cyclic loading even when its initial formation stiffness is slightly lower than that of the ballast.
- The amplitudes of the track displacements were higher at the lower frequencies, i.e. the greater loads. Under cyclic loading the

amplitudes of the sleepers, in the case of the ballasted track test, were nearly 20 times higher than those of the concrete slab track test.
- In the cyclic/dynamic tests a change in the amplitude of the actuator stroke after millions of loading cycles was observed. The amplitudes slightly declined due to the stiffness increase in the substructure indicating plastic settlement during shakedown.

In terms of high-speed lines some general observations can be made. The ballast did reach a resilient state under cyclic loading but the level of settlement required to achieve this (even with a high stiffness formation) would result in track geometry correction (e.g. tamping) to prevent high passenger vertical acceleration levels (e.g. 2.5% of g for very high speed trains). If tamping were used to correct the geometry the ballast would again be disturbed and hence settle, generating the constant need for track maintenance to ensure that passenger acceleration levels are within allowable limits. The effect is greatly reduced for concrete slab track, but in this track type the significant issue is ensuring that the ground does not settle otherwise the concrete slab may become damaged.

Acknowledgments

The authors are grateful to the Engineering and Physical Sciences Research Council (EPSRC) for funding this work under Grant Number EP/N009215/1. Tarmac, Tensar and Max-Bögl are also acknowledged for their support with regards to the experimental testing stages.

Appendix A. Supplementary material

Supplementary data associated with this article can be found, in the online version, at https://doi.org/10.1016/j.trgeo.2018.08.003.

References

[1] Bian X, Jiang H, Cheng C, Chen Y, Chen R, Jiang J. Full-scale model testing on a ballastless high-speed railway under simulated train moving loads. Soil Dyn Earthquake Eng 2014;66:368–84.
[2] Woodward P, Kennedy J, Laghrouche O, Connolly D, Medero G. Study of railway track stiffness modification by polyurethane reinforcement of the ballast. Transp Geotech 2014;1(4):214–24.
[3] Chen R, Zhao X, Wang Z, Jiang H, Bian X. Experimental study on dynamic load magnification factor for ballastless track-subgrade of high-speed railway. J Rock Mech Geotech Eng 2013;5(4):306–11.
[4] Anderson WF, Key AJ. Model testing of two-layer railway track ballast. J Geotech Geoenviron Eng 2000;126(4):317–23.
[5] Brough MJ, Ghataora G, Stirling AB, Madelin KB, Rogers CD, Chapman DN. Investigation of railway track subgrade. Part 2: Case study. Proceedings of the institution of civil engineers-transport. Thomas Telford Ltd.; 2006. p. 83–92. no. 2.
[6] Pita AL, Teixeira PF, Robusté F. High speed and track deterioration: the role of vertical stiffness of the track. Proc Inst Mech Eng, Part F: J Rail Rapid Transit 2004;218(1):31–40.
[7] Colaço A, Costa PA, Connolly DP. The influence of train properties on railway ground vibrations. Struct Infrastruct Eng 2016;12(5):517–34.
[8] Bian X, Jiang H, Chen Y. Accumulative deformation in railway track induced by high-speed traffic loading of the trains. Earthq Eng Eng Vibrat 2010;9(3):319–26.
[9] Selig ET, Waters JM. Track geotechnology and substructure management. Thomas Telford; 1994.
[10] Thom N, Oakley J. Predicting differential settlement in a railway trackbed. In: Proceedings of railway foundations conference: Railfound, vol. 6; 2006. p. 190–200.
[11] Indraratna B, Ngo NT, Rujikiatkamjorn C. Deformation of coal fouled ballast stabilized with geogrid under cyclic load. J Geotech Geoenviron Eng 2012;139(8):1275–89.
[12] Alva-Hurtado J, Selig E. Permanent strain behavior of railroad ballast. In: Proceedings of the international conference on soil mechanics and foundation engineering, vol. 1; 1981. p. 543–6.
[13] Shenton M. Ballast deformation and track deterioration. Track Technol 1985:253–65.
[14] Sato Y. Japanese studies on deterioration of ballasted track. Veh Syst Dyn 1995;24(suppl. 1):197–208.
[15] Dahlberg T. Some railroad settlement models—a critical review. Proc Inst Mech Eng, Part F: J Rail Rapid Transit 2001;215(4):289–300.
[16] Abadi T, Le Pen L, Zervos A, Powrie W. A review and evaluation of ballast settlement models using results from the Southampton Railway Testing Facility (SRTF). Procedia Eng 2016;143:999–1006.
[17] Hufenus R, Rueegger R, Banjac R, Mayor P, Springman SM, Brönnimann R. Full-scale field tests on geosynthetic reinforced unpaved roads on soft subgrade. Geotext Geomembr 2006;24(1):21–37.
[18] Lekarp F, Dawson A. Modelling permanent deformation behaviour of unbound granular materials. Constr Build Mater 1998;12(1):9–18.
[19] Xiao Y, Zheng K, Chen L, Mao J. Shakedown analysis of cyclic plastic deformation characteristics of unbound granular materials under moving wheel loads. Constr Build Mater 2018;167:457–72.
[20] ASTM-D2487-17. Standard Practice for Classification of Soils for Engineering Purposes (Unified Soil Classification System), ed. West Conshohocken, PA: ASTM International; 2017.
[21] ZTVE-StB. Surface covering dynamic compaction methods - German specifications and regulations. Additional technical contractual conditions and guidelines for earthwork in road construction and technical instructions for soil and rock in road construction, ed; 1994.
[22] DIN-18134. Determination of deformation and strength characteristics of soil by the plate loading test. Deutsche Norm., ed; 1999.
[23] Brown S, Brodrick B, Thom N, McDowell G. The Nottingham railway test facility, UK. Proceedings of the institution of civil engineers-transport. Thomas Telford Ltd.; 2007. p. 59–65. no. 2.
[24] Sharpe P, Brough M, Dixon J. Geogrid trials at Coppull Moor on the West Coast main line. Proc. of 1st Int. Conf. on Railway Foundations–RailFound06 (11.09-13.09. 2006). Birmingham: University of Birmingham Publ; 2006. p. 367–75.
[25] Kouroussis G, Connolly DP, Verlinden O. Railway-induced ground vibrations–a review of vehicle effects. Int J Rail Transport 2014;2(2):69–110.
[26] Takemiya H, Bian X. Substructure simulation of inhomogeneous track and layered ground dynamic interaction under train passage. J Eng Mech 2005;131(7):699–711.
[27] Woodward PK, Laghrouche O, Mezher SB, Connolly DP. Application of coupled train-track modelling of critical speeds for high-speed trains using three-dimensional non-linear finite elements. Int J Railway Technol 2015;4(3).
[28] Mezher SB, Connolly DP, Woodward PK, Laghrouche O, Pombo J, Costa PA. Railway critical velocity–Analytical prediction and analysis. Transp Geotech 2016;6:84–96.
[29] Fair P. The geotechnical behaviour of ballast materials for railway track maintenance PhD Thesis University of Sheffield; 2004.
[30] Kwan CCJ. Geogrid reinforcement of railway ballast. University of Nottingham; 2006.
[31] Aursudkij B. A laboratory study of railway ballast behaviour under traffic loading and tamping maintenance. University of Nottingham; 2007.